Tellus (2001), 53A, 368–379
Printed in UK. All rights reserved

TELLUS
ISSN 0280–6495

A Lagrangian computation of stratosphere–troposphere exchange in a tropopause-folding event in the subtropical Southern Hemisphere

By J. MELOEN*, P. C. SIEGMUND and M. SIGMOND, *Royal Netherlands Meteorological Institute (KNMI), PO Box 201, 3730 AE De Bilt, The Netherlands*

(Manuscript received 31 January 2000; in final form 20 November 2000)

ABSTRACT

A new Lagrangian technique to calculate the air mass flux across potential vorticity (Q) surfaces has been used to perform a case study of a tropopause-folding event in the subtropical Southern Hemisphere. The flux is computed from the rate of change in Q along trajectories, which are calculated from ECMWF wind data. Because the tropopause can be defined as a Q surface, the method can be used for the calculation of stratosphere–troposphere exchange (STE). A large number of forward and backward trajectories were calculated, starting in the vicinity of the tropopause fold. This fold was observed during the TRACAS (TRAnsport of Chemical species Across the Subtropical tropopause) experiment at La Reunion (21°S, 55°E) in July 1998. With the Lagrangian method the cross tropopause air mass flux can be calculated for the different tropopause levels, that occur in case of a tropopause folding. The computed mass exchange is about -20×10^{13} kg (i.e., downward) in 4.5 days, which is rather small compared to other (midlatitude) mass exchange studies. The ratio of the fluxes per unit of area in and outside of the fold is about 200 : 1. An indication of the accuracy of the calculated fluxes has been obtained with the help of the ozone soundings made during the TRACAS experiment.

1. Introduction

Stratosphere–troposphere exchange (STE) is one of the main processes controlling the impact of man's activities on atmospheric composition and climate forcing (Holton et al., 1995). Despite this importance, there exist no accurate estimates of STE. This is particularly true for estimates that are limited in space and time. Various versions of a general formula derived by Wei (1987) are often used to calculate mass exchange between the troposphere and the stratosphere. These calculations, however, suffer from cancellation of large terms (Wirth and Egger, 1999).

Wirth and Egger (1999) compared in their study 5 methods to diagnose mass exchange across the tropopause, 3 of which were derived from Wei's general formula, in one method the flux was evaluated directly as the difference between the motion of the air and the motion of the tropopause, and one method involved the calculation of a large number of trajectories. Their trajectory method yielded reasonable estimates for the cross-tropopause mass flux, together with Wei's general formula with potential vorticity (Q) as vertical coordinate. Disadvantage of the latter method is that the potential vorticity sources and sinks need to be estimated explicitly.

Siegmund et al. (1996) calculated STE with wind and temperature data at high spatial and temporal resolution. They found that the diagnosed instantaneous and local cross tropopause fluxes do not notably depend on the horizontal

* Corresponding author.
e-mail: meloen@knmi.nl

and temporal resolution if these becomes higher than, respectively, 1° latitude/longitude and 6 h. A resolution decrease to 3.75° and 12 h, however, generally leads to quite different results for the local and instantaneous fluxes.

With previous methods the tropopause in tropopause foldings is generally truncated to a single level (Wei, 1987). This is mostly done for technical reasons, because the methods are not capable of dealing with multiple tropopauses. The consequence of this truncation is that any stratospheric air entering the fold is assumed to be irreversibly transferred to the troposphere. The accuracy of this assumption however has never been investigated. With the Lagrangian method applied in this study all, possibly multiple, tropopause levels are taken into account.

In the present study Wei's general formula with potential voricity as vertical coordinate is used, and the terms in this formula are determined with the help of trajectories, which are calculated at a high spatial and temporal resolution. Wirth and Egger (1999) used their trajectories to calculate the difference in tropopause pressure and trajectory pressure at the endpoint of the trajectory, and took this as a measure for the STE in the considered time interval. Sigmond et al. (2000) developed the Lagrangian method used in the present study for the calculation of STE. Sigmond et al. (2000) concentrated on the statistical significance of the method and its application to an extratropical cyclone. In the present study the method is applied to a subtropical tropopause folding which was observed in the Southern Hemisphere during the TRACAS (TRansport of Chemical species Across the Subtropical tropopause) experiment. This experiment took place at the subtropical island La Reunion (21°S, 55°E). The method is evaluated with the help of TRACAS ozone soundings.

Tropopause folds in the Southern Hemisphere subtropics are believed to differ in some important aspects from the more frequently studied folds in the Northern Hemisphere midlatitudes (Ramond et al., 1981). Tropopause folds near the subtropical jet are e.g., believed not to penetrate as deep into the troposphere in comparison with midlatitude folds, since the frontal zone is broader and the tropopause is less steeply folded (Gouget et al., 1996). Therefore, the exchange can expected to be less in subtropical folds compared to midlatitude folds. The fold examined in this study is thought to be associated with the Hadley circulation (Baray et al., 2000). This is also an indication that care must be taken when comparing the fold of this study with Northern Hemisphere midlatitude folds.

In Section 2 the method to calculate the cross Q air mass flux is explained, and a description is given of the trajectory model, its input data and the observations made during the TRACAS experiment. In Subsection 3.1 the reliability of the calculated cross Q air mass flux F is investigated. This section is divided in two parts. In Subsection 3.1.1 a qualitative evaluation is done to analyse the geographical variability of the flux. In Subsection 3.1.2 a quantitative evaluation is done to investigate the reliability of the magnitude of the computed fluxes. Finally, in Subsection 3.2, the computed area- and time-integrated flux is presented.

2. Method and data

In this section, first an explanation is given how the cross potential vorticity air mass flux (F) is derived. Next a description is given of the wind and temperature data used for the calculation of F, and the trajectory model is described. Finally a description is given of the TRACAS experiment, from which the ozone soundings are used in this study.

2.1. *The flux calculation*

For the calculation of the air mass flux F across a potential vorticity surface the general equation derived by Wei (1987) is used. With potential vorticity (Q) as the vertical coordinate, this general formula becomes particularly simple and can be written as:

$$F = -\frac{1}{g}\frac{\partial p}{\partial Q}\frac{\mathrm{d}Q}{\mathrm{d}t}, \qquad (1)$$

where g is the acceleration due to gravity, p is pressure, Q potential vorticity and t is time. The unit of F is $\mathrm{kg\,m^{-2}\,s^{-1}}$.

The formula as given by Wei (1987) is strictly valid only for cases where $|Q|$ increases monotonously with height. It does not correctly describe the case of multiple dynamical tropopauses. If the tropopauses are numbered from the top of the atmosphere downward, a negative flux given by the Wei formula is from the stratosphere downward at odd numbers and from troposphere upward at even numbers of the tropopause. In order to take care that negative values of F are always from the stratosphere to the troposphere, F is written as:

$$F = \frac{1}{g}\left|\frac{\partial p}{\partial Q}\right|\frac{\mathrm{d}Q}{\mathrm{d}t}. \tag{2}$$

The method used in this study to compute F has been described by Sigmond et al. (2000), and is summarized below. At the gridpoint where the flux F is to be determined, a 6 h forward and a 6 h backward trajectory is calculated. These trajectories are started on the tropopause every 12 h, on a grid with $1 \times 1^\circ$ resolution. Along these trajectories Q and $\partial p/\partial Q$ are calculated. Because the instantaneous $\mathrm{d}Q/\mathrm{d}t$ is very noisy, a linear least square regression of Q along the 12-h trajectory versus time is made, of which the slope is used as an approximation of the 12-h mean $\mathrm{d}Q/\mathrm{d}t$. F is then approximated as

$$F \approx \frac{1}{g}\overline{\left|\frac{\partial p}{\partial Q}\right|}^{12\,\mathrm{h}}\overline{\frac{\mathrm{d}Q}{\mathrm{d}t}}^{12\,\mathrm{h}}, \tag{3}$$

where $\overline{|\partial p/\partial Q|}^{12\,\mathrm{h}}$ is the averaged absolute $\partial p/\partial Q$ along the 12-h trajectory.

In this study the tropopause is defined as a Q surface. Q values are generally negative in the Southern Hemisphere, so that absolute values have to be taken to make them comparable with Northern Hemisphere Q values. In the midlatitudes the tropopause is defined by a $|Q|$ value of typically 2 PVU ($1\ \mathrm{PVU} = 10^{-6}\ \mathrm{K\ m^2\ kg^{-1}\ s^{-1}}$). The most suitable $|Q|$ value to define the tropopause depends on the season and the region under consideration (Folkins and Appenzeller, 1996; Grewe and Damaris, 1995). A value of 1.5–2.5 PVU seems to be a reasonable range for the $|Q|$ of the subtropical tropopause. Therefore, trajectories are started at three different Q levels, i.e., -1.5, -2 and -2.5 PVU. The derived flux is attributed to the starting point and time of these trajectories. Negative values of F correspond to fluxes towards lower values of $|Q|$, i.e., towards the troposphere. Positive values correspond to fluxes in the opposite direction, i.e., towards the stratosphere.

In this study a folding event is identified when the Q surfaces are truly folded, i.e., when the same Q value can be found three times at one gridpoint at different altitudes. For each such gridpoint, trajectories are started and F is calculated at the 3 different altitudes. From the uppermost level downward these fluxes are called F_1, F_2 and F_3 (Fig. 5). This means that F_1 always exists, but F_2 and F_3 are only nonzero in the case of a folding event. By adding these three separate values, the total flux, $F_{\mathrm{tot}} \equiv F_1 + F_2 + F_3$, for that gridpoint is obtained.

The above method becomes unreliable if $\partial p/\partial Q$ becomes large. This occurs for instance when the tropopause is steep (Lamarque and Hess, 1994). Therefore, fluxes with absolute values larger than $0.05\ \mathrm{kg\ m^{-2}\ s^{-1}}$ are considered to be unreliable, and are not taken into account. The threshold value of $0.05\ \mathrm{kg\ m^{-2}\ s^{-1}}$ was chosen on the basis of the probability density function of F given by Siegmund et al. (1996). For the extratropical Northern Hemisphere, the absolute values of F hardly ever exceed $0.05\ \mathrm{kg\ m^{-2}\ s^{-1}}$. Although the present study concentrates on a Southern Hemisphere subtropical fold, the range of values is not expected to be larger than the range for Northern Hemisphere values (Gouget et al., 1996). If one of the separate fluxes F_1, F_2 or F_3 is not taken into account, then also F_{tot} is not taken into account. This is the case in less than 1% of the total area.

2.2. The ECMWF data

As input to the trajectory model ECMWF first guess wind and temperature data are used. These data are available on a $1^\circ \times 1^\circ$ grid, obtained from the T213 spectral resolution of the ECMWF model, and at 31 vertical levels. Around the tropopause the vertical resolution is about 25 hPa. The temporal resolution of the data is 6 h.

For the comparison of the data with measurements, first guess data are used rather than analyses. This is because the latter are not physical consistent due to the addition of observations to the model data. An advantage of forecast data would have been that the data remain physical consistent during the entire trajectory computation. But the differences between a 5-day forecast and the analysis are too large to justify this approach.

2.3. *The trajectory model*

For calculating the trajectories, the KNMI trajectory model is used as described by Scheele et al. (1996). This model calculates the 3-dimensional displacement of air parcels for each timestep using the iterative scheme after Petterssen (1940). In the present study the trajectory time step is 10 min. Spatial interpolation (linear in longitude, latitude and the logarithm of pressure) and temporal interpolation (quadratic) are applied to the input data to obtain the wind at the trajectory locations. In this study, 3-dimensional rather than isentropic trajectories are calculated in order to include diabatic effects in the calculations of the cross Q air mass flux. For winds from ECMWF, 3-dimensional trajectories are generally more accurate at tropopause heights than isentropic trajectories, as is found, e.g., by Stohl and Seibert (1998). To calculate Q at location X and at time t, Q is first calculated at location X at the three 6-h ECMWF first guess times closest to time t, and is then quadratically interpolated to time t.

2.4. *The TRACAS experiment*

In July 1998, a measurement campaign called TRACAS (TRAnsport of Chemical species Across the Subtropical tropopause) was held in the Indian Ocean region to collect ozone observations near the Southern Hemispheric subtropical jet stream. One of the objectives was to study how the dynamical processes associated with the subtropical jet control the exchange of chemical species through the tropopause. During the experiment, amongst others, ozone sondes were launched, at La Reunion Island (21°S, 55°E). During the whole of July 1998 a tropopause fold persisted over a considerable longitude range from the mid-Atlantic to the mid-Pacific, i.e., from 0° to 200°E, and from 20° to 35°S. The fold is thought to be associated with the Hadley circulation (Baray et al., 2000). In this study the time interval is restricted to the part of the period when the fold was quite pronounced and over La Reunion, i.e., from 0000 GMT 14 July 1998 to 1200 GMT 18 July 1998. Fluxes are calculated for the area between 0° to 160°E and 10° to 50°S. In the selected period 4 ozone sondes were launched, from which the sondes on 1000 and 1800 GMT of 17 July 1998 are used for the purpose in this study, thanks to the small time interval between them.

3. Results

In this section, the results of the exchange in the tropopause fold, calculated with the method described in Subsection 2.1 is presented. In Subsection 3.1, first an evaluation is done to investigate the accuracy of the calculated cross Q air mass flux. This section is divided in two parts, the first is the investigation of the geographical distribution, the second is a quantitative evaluation of the flux with the help of ozone soundings. In Subsection 3.2 the results are given of the time and area integrated air mass flux through the various Q levels and the various tropopause regions inside and outside the tropopause fold.

3.1. *Evaluation of F*

3.1.1. Geographical distribution of F. In Fig. 1 the total flux (F_{tot}) is given for the -1.5 PVU level on 1200 GMT 17 July 1998, overlaid with the $|Q|$ on the 300 hPa surface. The tropopause fold and two upper level troughs can be distinguished by the contouring of Q, which indicates regions where the Q surfaces are located at a lower than normal position. The fold can be found from 25° to 35°S along a large part of the longitude range, and the two upper level troughs are located from 20° to 55°E and from 100° to 120°E both below 40°S. The two upper level troughs can also be distinguished on figures of mean sea level pressure (not shown). As can be seen in Fig. 1 high values of the flux are found in the tropopause fold and in the upper level troughs, as would be expected (Wirth and Egger, 1999; Lamarque and Hess, 1994). In most other regions the flux is very small. Typical values found for the calculated air mass flux are of the order 0.02 kg m^{-2} s^{-1}. This is comparable with the magnitude found by Siegmund et al. (1996). However, Wirth and Egger (1999) found values of an order 5 larger in a cut off low event at NH midlatitudes. These fluxes might be larger because of the different physical mechanisms of decay in a cut off low event and the difference in place where the event occured, compared with the tropopause fold studied here. From this the conclusion can be drawn that the method used here to calculate the cross Q air mass

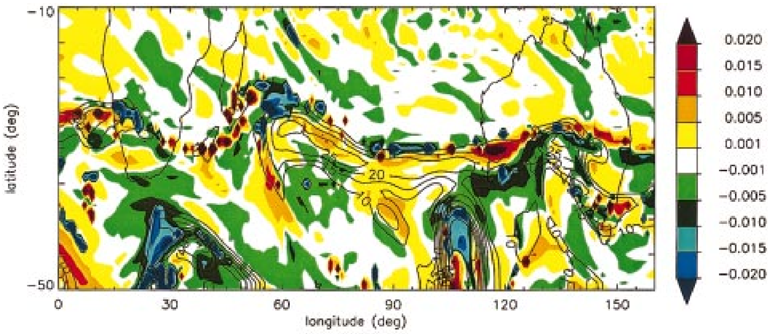

Fig. 1. Longitude/latitude plot for the total air mass flux (F_{tot}, in units of kg m^{-2} s^{-1}) across the -1.5 PVU surface (colour plot), overlaid with Q (in units of -0.1 PVU) on the 300 hPa surface (contour lines), both on 1200 GMT 17 July 1998. Positive values of F correspond to fluxes towards higher, more stratospheric levels of $|Q|$, negative values correspond to fluxes in the opposite direction. The contours of Q indicate regions where the Q surfaces are located at a lower than normal position, as is the case in the upper level troughs and in tropopause foldings. These high values of Q at 300 hPa correspond to the largest fluxes.

flux is capable of detecting the areas where exchange is expected to occur and that the order of magnitude of the fluxes is in the range of what is expected.

In Fig. 2 the fluxes through the different parts of the tropopause fold are displayed for the -1.5 PVU level on 1200 GMT 17 July 1998. From these figures it can be seen that the exchange in the fold takes mainly place in the middle (F_2) and lower (F_3) parts of the fold. As can be anticipated multiple tropopauses are not found for upper level troughs, and hence here large fluxes are only found for F_1. Often regions with positive and negative fluxes are found close to each other. The reason is that small scale mixing processes lead to bidirectional fluxes (Lamarque and Hess, 1994).

It is expected that particularly in tropopause folds the exchange is related to turbulent mixing of Q due to vertical windshear (Shapiro, 1980), instead of exchange by latent heating which is important in cut off lows (Wirth and Egger, 1999). Therefore, it is expected that in the regions with large windshear the flux will generally be large. The locations of the maximum in vertical windshear, at both sides of the maximum in windspeed, along the -1.5 PVU surface in Fig. 3 are located between 20° and 27°S. When comparing this with the location of the maximum in the total flux in Fig. 1 it is obvious that these areas coincide. This is another indication that the applied method is capable of detecting the areas where for physical reasons the exchange is expected to be large.

The same characteristics were found for the air mass fluxes across the -2.0 and -2.5 PVU surfaces (not shown), except for the size of the area where F_2 and F_3 are nonzero. This area decreases at higher $|Q|$ values, as can be expected from the structure of tropopause foldings (Fig. 5).

In summary, the analysis of the geographical variability of the calculated flux shows that the regions where the largest fluxes occur closely correspond to locations where STE would be expected for physical reasons.

3.1.2. Quantitative evaluation of the magnitude of F. In Subsection 3.1.1 it was shown that the geographical distribution of the calculated air mass fluxes looks reasonable. Another important aspect to know is whether the magnitude of the computed fluxes corresponds to what would be expected. As follows from eq. (1), uncertainties in F depend on uncertainties in $\partial p/\partial Q$ and dQ/dt. We will focus the attention on the uncertainty in dQ/dt, which is expected to dominate the uncertainty in F. The dQ/dt as computed in this study from trajectories, must be interpreted as the rate of change of the mean Q of a moving air parcel with a size of about the gridbox-size of the applied circulation data. This dQ/dt strongly depends on the subgrid-scale mixing of air masses with different Q values, which is implicitly parameterised in

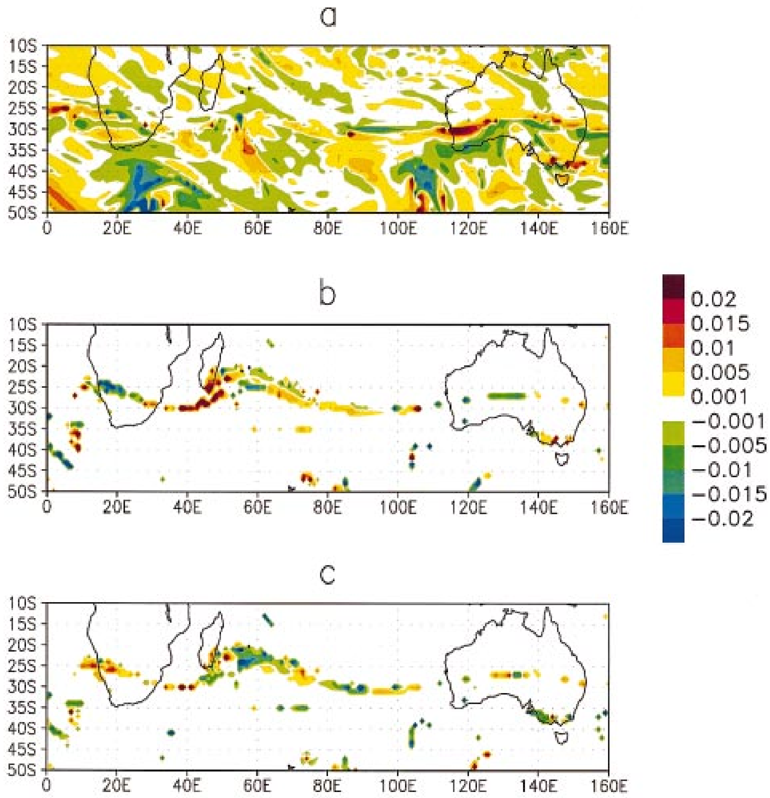

Fig. 2. The calculated cross Q air mass flux (in units of $\mathrm{kg\,m^{-2}\,s^{-1}}$) for 1200 GMT 17 July 1998 through the -1.5 PVU level. Fig. (a) represents the mass flux across the upper tropopause region (F_1 in Fig. 5), (b) through the middle tropopause region (F_2 in Fig. 5), and (c) through the lower tropopause region (F_3 in Fig. 5). The total mass flux ($F_{\mathrm{tot}} \equiv F_1 + F_2 + F_3$), is displayed in Fig. 1. F_2 and F_3 are nonzero only in the case of multiple tropopauses.

the ECMWF model. Although the subgrid-scale mixing is parameterised in terms of the model variables rather than Q, implicitly there is an effect on $\mathrm{d}Q/\mathrm{d}t$ via the dependence of Q on the modelled temperature and horizontal velocity. In addition, numerical diffusion adds to $\mathrm{d}Q/\mathrm{d}t$. If $\mathrm{d}Q/\mathrm{d}t$ would be zero, then the Q along trajectories would be constant and Q at the begin- and endpoints of the trajectories, Q_b and Q_e, would be the same. In other words, Q_e would be the result of advection of Q_b. In reality $\mathrm{d}Q/\mathrm{d}t$ is generally nonzero, and Q_e is the sum of Q_b and the $\mathrm{d}Q/\mathrm{d}t$ along the trajectory. The value of Q_e at some point x_0 and time t_0, $Q(x_0, t_0)$, can be computed from ECMWF data at t_0. The Q_b can be obtained by computing a back trajectory starting in (x_0, t_0) and ending in $(x_1, t_0 - \Delta t)$ and setting $Q_\mathrm{b} = Q(x_1, t_0 - \Delta t)$, which can be computed from ECMWF data at $x_1, t_0 - \Delta t$ (in this study Δt has a value of 6 h). In this section it is investigated whether Q_e is more realistic (to be defined below) than Q_b, or, in other words, whether the $\mathrm{d}Q/\mathrm{d}t$ along the trajectory improves Q_e or not. This might give some qualitative information about the accuracy of the modelled $\mathrm{d}Q/\mathrm{d}t$, and hence about the accuracy of the flux F. This investigation is done by considering two ozone and Q profiles at the same location, obtained from independent sources, at a time interval of several hours. It is assumed that during this short period the relation between ozone and Q is constant. For each point of the profiles both Q_e and Q_b are computed and it is determined whether the ozone–Q relation is more constant for Q_e or for Q_b. If it is more constant for Q_e, than it is assumed that the addition of the modelled $\mathrm{d}Q/\mathrm{d}t$ along the trajectory to Q_b results in a better

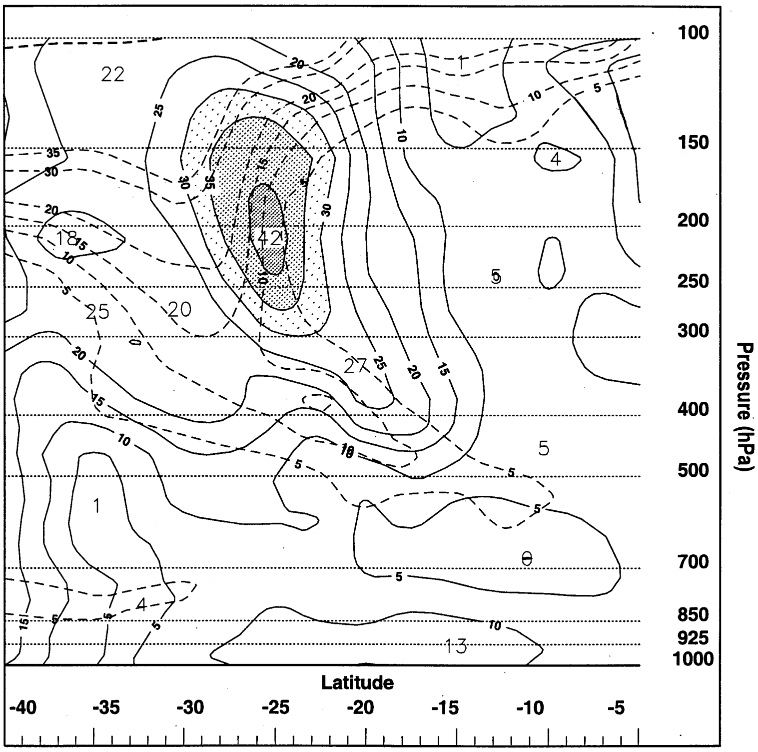

Fig. 3. Cross section at 55°E of the wind speed (m/s) for 1200 GMT 17 July 1998 (first guess model level data). Dashed lines denote values of Q (in units of -0.1 PVU), solid lines denote windspeed. As can be seen from this figure the largest windshear for the -1.5 PVU surface can be found between 20°S to 27°S, around the windspeed maximum. In the uppermost panel in Fig. 1 (F_{tot}) can be seen that here the largest values across the -1.5 PVU surface occur.

Q_e and, hence, that this dQ/dt is less or more realistic.

In Fig. 4 the solid and dashed lines show the values of ozone versus $|Q_e|$ along a vertical profile above La Reunion at times t_1 and t_2, where $t_1 = 1000$ GMT 17 July 1998, and $t_2 = t_1 + 8$ h. These Q_e values, hereafter denoted by Q_{e1} and Q_{e2}, have been computed from ECMWF data at t_1 and t_2 for the levels at which these data are available (see Subsection 2.2). The measured ozone values have been averaged over the layers to which these levels apply. Both the solid and the dashed line shows the presence of a tropopause fold: following the lines from 30 ppbv to the right in the figure, which corresponds to going up in the atmosphere, the ozone values increase to about 75 ppbv in the centre of the fold, then decrease (following the lines to the left) to about 50 ppbv in the troposphere between the fold and the stratosphere, and finally increase to more than 100 ppbv at stratospheric levels. Also the profiles of Q_{b1} and Q_{b2} have been determined, by computing 6 h back trajectories starting at the different levels above La Reunion at, respectively, $t = t_1$ and $t = t_2$, and setting Q_b equal to the Q at $x_1, t_0 - \Delta t$, after a linear regression of Q versus time along the 6-h back trajectory. The values of ozone and $|Q|$ above La Reunion are shown by the dotted lines in Fig. 4.

According to Haynes and McIntyre (1990), "adiabatic mixing" does not exist. On the other hand they state that for most tropopause folds the diabatic changes in Q because of mixing will be small. Ravetta et al. (1999) also found that only in a small part of the fold diabatic mixing plays a role. Therefore, as a next step, it is assumed that during the period $[t_1, t_2]$ diabatic and frictional sources of Q and chemical sources of ozone can be neglected, which is a reasonable assumption

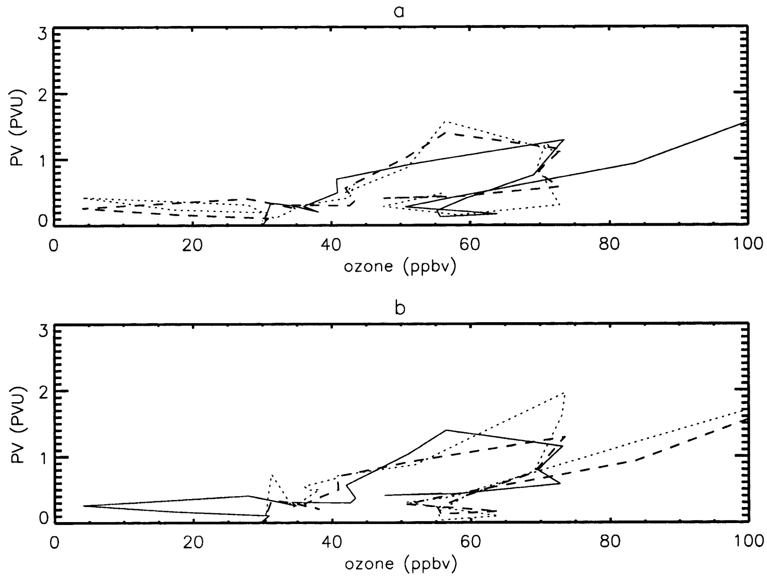

Fig. 4. Comparison of the relation between the absolute value of Q (in units of PVU) and ozone (in units of ppbv) at times t_1 and t_2 ($t_1 = 1000$ GMT 17 July 1998, $t_2 = t_1 + 8$ h), where $Q(t)$ has been computed either from ECMWF data at time t (denoted by Q_e) or from 6-h back trajectories starting at time t (denoted by Q_b). See the text for details. For (a) solid line $= Q_{e1}$, dashed line $= Q_{e2}$, dotted line $= Q_{b2}$. For (b) solid line $= Q_{e2}$, dashed line $= Q_{e1}$, dotted line $= Q_{b1}$.

for such a short time period. Under this assumption, mixing is the only "source" of the gridbox-averaged ozone and Q. Also it is assumed that within an air mass mixing does not affect the relation between ozone and Q, i.e., this relation is assumed to be linear (Plumb and Ko, 1992; Danielsen, 1990). In Fig. 4a, two different air masses can be identified in which at t_1 and t_2 the ozone–Q_e relation is more or less the same (i.e., where the dashed line is relatively close to the solid line): below and above the ozone maximum in the fold. This similarity might imply that the change between t_1 and t_2 is mainly due to advection. However, it is also possible that there is substantial mixing. In that case the similarity would imply that the mixing is parameterized reasonably well in the ECMWF model. Fig. 4a shows that there is indeed substantial mixing, since there are substantial differences of about 10%, between Q_{e2} and Q_{b2}. In addition, the difference between Q_{e2} and Q_{e1}, averaged over the fold from 45 ppbv to the ozone maximum and back to 50 ppbv, is 0.2 PVU, whereas the difference between Q_{b2} and Q_{e1} is about 50% larger. Hence, the invariance of the ozone–Q relation is improved by the mixing (which determines the difference between Q_{b2} and Q_{e2}). This result improves our confidence in the accuracy of the computed $\mathrm{d}Q/\mathrm{d}t$, and of the related magnitude of F. The same conclusion applies to Fig. 4b, in which Q_b has been determined for the Q-profile at t_1.

3.2. *Exchange in the fold: time and area integration*

In order to evaluate the flux for various Q surfaces, outside the fold and through the different parts of the fold, and to intercompare the exchange of air inside and outside the fold, the fluxes are integrated over time and space. The result is shown in Fig. 5. The time period over which the integration is performed is from 0000 GMT 14 July 1998 to 1200 GMT 18 July 1998 and the considered area is from 35° to 120°E and from 15° to 40°S. The flux has been integrated for the Q levels of -1.5, -2.0 and -2.5 PVU, and for the separate fluxes, i.e., F_1 (through the upper part of the fold), F_2 (through the middle part) and F_3 (through the lower part) and F_{tot} (the total flux).

In the fold the net exchange is largest in its lower part (F_3). In the upper part (F_1), the

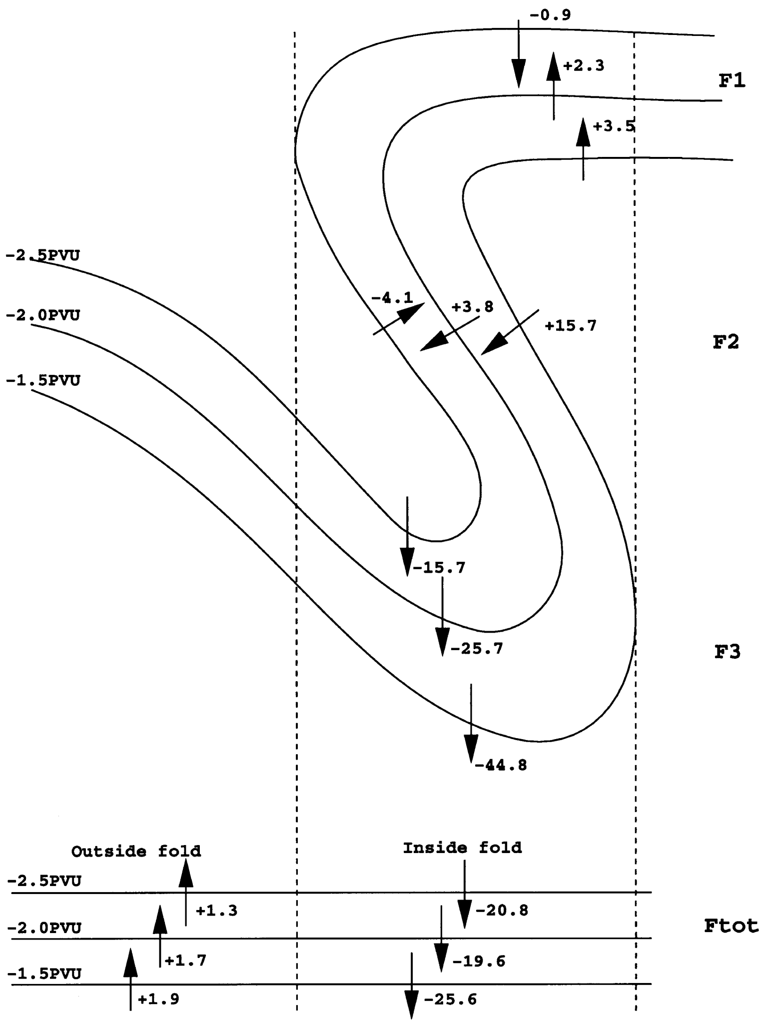

Fig. 5. Time (0000 GMT 14 July 1998–1200 GMT 18 July 1998) and area (35°–120°E/15°–40°S) integrated mass flux across the -1.5, -2 and -2.5 PVU surfaces ($\times 10^{13}$ kg). The upper part of the figure displays the integrated flux through the different tropopause regions in the fold, the lower part displays the total mass flux ($F_{tot} = F_1 + F_2 + F_3$) inside and outside the fold. On 1200 GMT 17 July 1998 10% of the area was covered by the fold.

exchange is small, but still larger then outside the fold. The net exchange in the middle part of the fold (F_2) is about 3–5$\times$ smaller than in the lower part. This is in agreement with Shapiro (1980), who also found the largest exchange in the lower part of the fold.

A striking feature is that for F_2 and for F_1, inside the fold, opposite signs are found for the cross Q air mass flux through the various Q levels. This might be because the windshear maximum is found in this area, and the exchange can be expected to be bidirectional. This is in agreement with Ravetta et al. (1999), who showed that the turbulent heat flux in the vicinity of large wind shear around the jet core, which is situated at the middle part of the fold, is responsible for exchange towards the stratosphere. In the lowest part of the fold the exchange is directed towards the troposphere. Outside the tropopause fold the net exchange is directed towards the stratosphere.

In the fold the value for the net F_{tot} is -20×10^{13} kg, whereas in the area outside the fold the value is about 1×10^{13} kg. About 10% of the area was covered by the fold, therefore it follows from these values that the ratio of the fluxes per unit of area in and outside of the fold is about 200:1.

The net mass exchange for the total area is about -20×10^{13} kg in 4.5 days for all three Q surfaces. Not much studies of mass exchange have been performed in the subtropics yet. Compared to midlatitude studies this estimate is closest to the studie of Vaughan et al. (1994), who estimated a mass exchange of around -20×10^{13} kg in 1.5 days. Compared to other midlatitude studies the estimate of our study is rather small; e.g., Lamarque and Hess (1994) found a net mass exchange of -4.9×10^{14} kg in 4 days, Reiter and Mahlman (1965) found -6×10^{14} kg in 2 days and Reiter et al. (1969) -4.8×10^{14} kg in 4 days. These larger fluxes in the midlatitudes are in agreement with Gouget et al. (1996), although from the lack of studies in the subtropics it cannot be said how much smaller the exchange can be expected to be in the subtropics.

It would be interesting to consider the difference in magnitude between the integrated fluxes in the lower and middle part of the fold, and to see why the integrated fluxes in the upper part of the fold and outside the fold are small. Therefore, in Fig. 6 the probability density function is given for the local instantaneous values of F_1 for the total area where the flux was calculated for (0–160°E, 10–50°S), and for F_2 and F_3 in the tropopause fold. This figure shows that the distribution for F_1 has a smaller width and a larger symmetry than the distributions for F_2 and F_3. As a consequence, the integrated flux for F_1 is smaller than those of F_2 and F_3. For F_2 and F_3 the difference between the probability density functions is not as large as might be expected from the difference in magnitude in the net mass exchange of Fig. 5, but it is clear that the distribution for F_3 is more asymmetric in such a way that a larger percentage of the values has a negative sign than for the distribution of F_2.

The distribution in Fig. 6a can be compared with the distribution given by Siegmund et al. (1996). The mean values of the upward and downward F of the latter distribution are, respectively, 2.66×10^{-3} kg m^{-2} s^{-1} and -2.73×10^{-3} kg m^{-2} s^{-1}. The values found in this study are, respectively, 2.23×10^{-3} kg m^{-2} s^{-1} and -2.54×10^{-3} kg m^{-2} s^{-1}. A narrower distribution in the present results might be due to less noise, compared to the results obtained by Siegmund et al. (1996). Another reason could be that the two results are not completely comparable because the midlatitudes are also taken into account in the study of Siegmund et al. (1996), where the exchange is expected to be larger.

4. Discussion and conclusions

In this work a Lagrangian method to calculate the air mass flux across Q surfaces is used for a Southern Hemisphere subtropical tropopause folding event above the Indian Ocean. A qualitative evaluation is performed to evaluate the geographical distribution of the calculated flux and a quantitative evaluation is performed to evaluate the magnitude of the flux for this tropopause folding case.

The results show that the largest fluxes are calculated in areas where the largest exchange is expected, i.e., in tropopause folds and upper level troughs, and that outside these areas the exchange is small. The largest fluxes occur in regions with strong vertical windshear. In the fold the largest fluxes are found for the lowermost tropopause region. Positive and negative numbers are found close to each other, at locations where small scale mixing is expected, leading to bidirectional exchange.

What could be the case for the method applied here is that the values found for the air mass flux might become erroneously large near steep surfaces, where the term $\partial p/\partial Q$ becomes large. This is particularly the case for F_2 and F_3. To investigate this, the % of calculated fluxes which are not taken into account, i.e., which are larger than 0.05 or smaller than -0.05 kg m^{-2} s^{-1}, are calculated. The percentage of values not taken into account is about 10% for F_2 and F_3, and less than 1% over the total area. When taking an even higher threshold of 0.1 kg m^{-2} s^{-1}, less than 1% of F_2 and F_3 is not taken into account. Hence, the problem of erronously large values of $\partial p/\partial Q$ exists only in a small part of the total area.

Compared to other methods, it is found that the probability density function of the fluxes calcu-

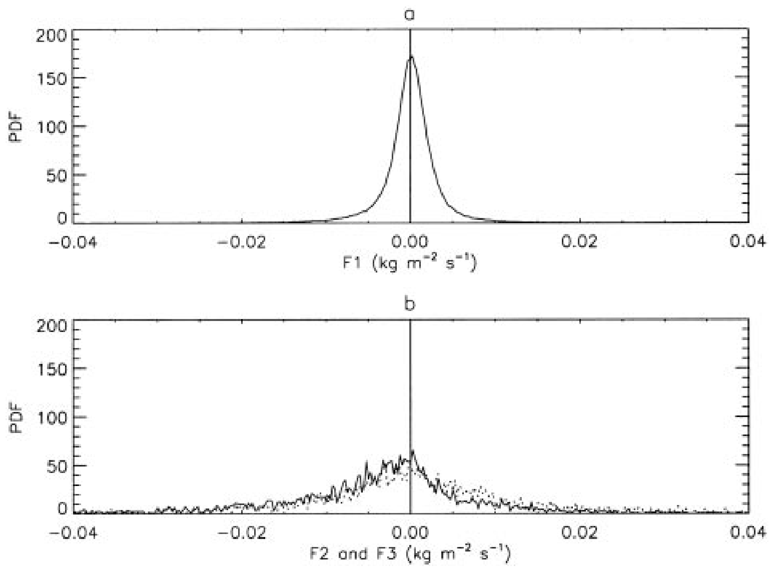

Fig. 6. Probability density functions of the local instantaneous values of F_1 (for 0–160°E to 10–50°S, upper panel), and of F_2 and F_3 (dotted and solid line, lower panel, respectively), both for the same 4.5 day period as in Fig. 5. On the x-axis F (in kg m^{-2} s^{-1}) is displayed. The interval over which the Fs are summed is 0.00025 kg m^{-2} s^{-1}

lated with the new method is narrower. This is believed to be an indication that the new method is more reliable because numerical noise is expected to be partly responsible for the tails of the distributions evaluated with the other techniques. On the other hand, it could be a consequence of the fact that fluxes are expected to be smaller in the subtropics.

Because Southern Hemisphere subtropical folds have not often been investigated, and because of the special case of this fold being linked to the Hadley circulation, it is difficult to compare the results of this study with former results. As far as can be concluded now from the quantitative evaluation, the magnitude of the calculated cross Q air mass fluxes are within the expected range of values. When comparing the Q/ozone relation for which the Q is derived directly from the ECMWF and the relation for which the Q is derived with the help of back trajectories (Fig. 4), it is found that the mixing included in the ECMWF model improves the invariance of the Q/ozone relation. This improves our confidence in the computed dQ/dt and the associated cross Q air mass flux. However, an intercomparison with other (trajectory) models or case studies would be useful.

5. Acknowledgements

We greatfully acknowledge M. P. Scheele, for his help on the trajectory model and P. F. I. van Velthoven for helpful discussions. Comments of 2 anonymous reviewers helped improve the manuscript, and were greatly appreciated. This study has been supported by the European Union TRACAS project, EU grant ENV4-CT97-0520.

REFERENCES

Baray, J.-L., Daniel, V., Ancellet, G. and Legras, B. 2000. Planetary-scale tropopause folds in the Southern subtropics. *Geophys. Res. Lett.* **27**, 353–356.

Danielsen, E. F. 1990. In defense of Ertel's potential vorticity and its general applicability as a meteorological tracer. *J. Atmos. Sci.* **47**, 2013–2020.

Folkins, I. and Appenzeller, C. 1996. Ozone and potential vorticity at the subtropical tropopause break. *J. Geophys. Res.* **101**, D13, 18787–18792.

Gouget, H., Cammas, J.-P., Marenco, A., Rosst, R. and Jonquières, I. 1996. Ozone peaks associated with a subtropical tropopause fold and with the trade wind inversion: a case study from the airborne campaign TROPOZ II over the Caribbean in winter. *J. Geophys. Res.* **101**, 25979–25993.

Grewe, V. and Damaris, M. 1995. Calculating the global mass exchange between stratosphere and troposphere. *Ann. Geophysicae* **14**, 431–442.

Haynes, P. H. and McIntyre, M. E. 1990. On the conservation and impermeability theorems for potential vorticity. *J. Atmos. Sci.* **47**, 2021–2031.

Holton, J. R., Haynes, P. H., McIntyre, M. E., Douglass, A. R., Rood, R. B. and Pfister, L. 1995. Stratosphere–troposphere exchange. *Rev. Geophys.* **33**, 403–439.

Lamarque, J. and Hess, P. G. 1994. Cross-tropopause mass exchange and potential vorticity budget in a simulated tropopause folding. *J. Atmos. Sci.* **51**, 2246–2269.

Petterssen, S. 1940. *Weather analysis and forecasting*. McGraw-Hill Book Company, Inc., pp. 221–223.

Plumb, R. A. and Ko, M. K. W. 1992. Interrelationships between mixing ratios of long-lived stratospheric constituents. *J. Geophys. Res.* **97**, 10145–10156.

Ramond, D., Corbin, H., Desbois, M., Szejwach, G. and Waldteufel, P. 1981. The dynamics of polar jet stream as depicted by the Meteosat WV Channel radiance Fields. *Mon. Wea. Rev.* **109**, 2164–2176.

Ravetta, F., Ancellet, G., Kowol-Santen, J., Wilson, R. and Nedeljkovic, D. 1999. Ozone, temperature, and wind field measurements in a tropopause fold: comparison with a mesoscale model simulation. *Mon. Wea. Rev.* **127**, 2641–2653.

Reiter, E. R. and Mahlman, J. D. 1965. Heavy radioactive fallout over the southern United States, November 1962. *J. Geophys. Res.* **70**, 4501–4520.

Reiter, E. R., Glasser, M. E. and Mahlman, J. D. 1969. The role of the tropopause in stratospheric–tropospheric exchange process. *Pure Appl. Geophys.* **75**, 185–218.

Scheele, M. P., Siegmund, P. C. and van Velthoven, P. F. J. 1996. Sensitivity of trajectories to data resolution and its dependence on the starting point: in or outside a tropopause fold. *Meteorol. Appl.* **3**, 267–273.

Shapiro, M. A. 1980. Turbulent mixing within tropopause folds as a mechanism for the exchange of chemical constituents between the stratosphere and troposphere. *J. Atmos. Sci.* **37**, 994–1004.

Siegmund, P. C., van Velthoven, P. F. J. and Kelder, H. 1996. Cross-tropopause transport in the extratropical northern winter hemisphere, diagnosed from high-resolution ECMWF data. *Q. J. R. Meteorol. Soc.* **122**, 1921–1941.

Sigmond, M., Meloen, J. and Siegmund, P. C. 2000. Stratosphere–troposphere exchange in an extratropical cyclone, calculated with a Lagrangian method. *Ann. Geophysicae* **18**, 573–582.

Stohl, A. and Seibert, P. 1998. Accuracy of trajectories as determined from the conservation of meteorological tracers. *Q. J. R. Meteorol. Soc.* **124**, 1465–1484.

Vaughan, G., Price, J. D. and Howells, A. 1994. Transport into the troposphere in a tropopause fold. *Q. J. R. Meteorol. Soc.* **120**, 1085–1103.

Wei, M.-Y. 1987. A new formulation of the exchange of mass and trace constituents between the stratosphere and troposphere. *J. Atmos. Sci.* **44**, 3079–3086.

Wirth, V. and Egger, J. 1999. Diagnosing extratropical synoptic scale straexchange: a case study. *Q. J. R. Meteorol. Soc.* **125**, 635–655.